DEVELOPMENT OF AN AUTOMATIC AIRFLOW CONTROL SYSTEM FOR PRECISION SPRAYERS BASED ON TREE CANOPY DENSITY

Md Sultan Mahmud[1,2], Azlan Zahid[3], Long He[1,*], Heping Zhu[4], Daeun Choi[5], Grzegorz Krawczy[6], Paul Heinemann[1]

[1] Department of Agricultural and Biological Engineering, Pennsylvania State University, University Park, Pennsylvania, USA.
[2] Department of Agricultural and Environmental Sciences, Tennessee State University, McMinnville, Tennessee, USA.
[3] AgriLife Research, Texas A&M University, Dallas, Texas, USA.
[4] Application Technology Research Unit, USDA ARS, Wooster, Ohio, USA.
[5] Department of Agricultural and Biological Engineering, University of Florida, Wimauma, Florida, USA.
[6] Department of Entomology, Pennsylvania State University, University Park, Pennsylvania, USA.
[*] Correspondence: luh378@psu.edu

HIGHLIGHTS

- A LiDAR-guided automatic airflow control system for precision sprayers was developed.
- Three models were built to measure the amount of airflow required for apple trees.
- The study confirmed that adjusting the fan inlet could control airflow penetration into tree canopies.
- Results suggest that the system can reduce spray drift and off-target losses.

ABSTRACT. *The airflow discharged from orchard airblast sprayers is a primary component for successfully carrying spray droplets to the target trees. Because of the variation in orchard tree canopies, control of the airflow to minimize off-target loss during spray application is essential. An automatic airflow control system for precision sprayers was developed to maximize spray droplet coverage on targets and minimize off-target loss while considering the tree canopy densities. The primary component of the system was an iris damper, which was designed as a retrofit attachment on the fan inlet of a three-point airblast intelligent sprayer. A 3D light detection and ranging (LiDAR) sensor was installed at the top of the sprayer to acquire the tree canopy data. A motor was employed to control the damper opening with a micro-controller. To develop the models required for automatic airflow control, field experiments were conducted at three canopy density orchards with different cultivars (GoldRush, Gala, and Fuji). A total of 15 trees (five trees from each cultivar) were randomly selected, and five different damper openings (openings 1, 2, 3, 4, and 5) were tested for each tree. Opening 1 represented the same air inlet as a traditional precision airblast sprayer, while openings 2, 3, 4, and 5 were the sequentially reduced air inlets of the sprayer. A canopy density measurement algorithm was scripted to measure the canopy point density of individual trees. Three models were built to show relationships between (1) tree canopy point densities and airflows; (2) canopy densities and damper openings; and (3) damper opening and motor steps. The combination of the two models (2 & 3) was used to assess the amount of airflow required for a specific canopy density. Field validations for medium and high-density trees showed that the system achieved adequate spray penetration at the top, middle, bottom, back-left, and back-right positions of the tree sections and reduced off-target loss at the ground and edge of next row sections using openings 4 and 2, respectively. However, the mechanical motion of the damper required 3 s to move from minimum to maximum opening, so the average canopy density was recommended to control the airflow. The overall results suggested that the automatic airflow control system could reduce spray drift and off-target losses and improve spray application efficiency in orchards.*

Keywords. *Automation, Canopy sensing, Fan inlet, Precision spraying, Variable rate application.*

Submitted for review on 30 November 2021 as manuscript number MS 14972; approved for publication as a Research Article by Associate Editor Dr. Jason Ward and Community Editor Dr. Garey Fox of the Machinery Systems Community of ASABE on 25 August 2022.

Mention of company or trade names is for description only and does not imply endorsement by the USDA. The USDA is an equal opportunity provider and employer.

The size and characteristics of orchard tree canopies vary significantly depending on growth stages, cultivars, production practices, and growing season lengths. Variations of tree canopy characteristics are very common among different aged trees and cultivars throughout the growing season in different orchard blocks. The high variability of canopy characteristics can even be possible within trees in the same orchard block (Colaço et al., 2019). Conventional sprays using air-assisted sprayers apply constant-rate chemicals to fruit trees with

little or no consideration of tree canopy characteristics, which results in either over or under dosing with non-uniform spray deposition distribution (Owen-Smith et al., 2019). Inefficient chemical applications cause spray drift and pose potential risks to human health, ecosystems, and the environment (Pivato et al., 2015).

To overcome these challenges, precision sprayers equipped with advanced sensors have been developed with the capability to include tree canopy characteristics in spray decisions. This capability is a large step forward toward improving spray technologies. The sensors calculate the size, shape, foliage density, and foliage volume of individual trees and then control the sprayers to apply an adjusted spray volume accordingly to match the canopy architecture. This new spray technology reduces off-target deposition and increases application efficiency (Zhang et al., 2018). Among these sensors are digital cameras, ultrasonic, and LiDAR. Digital cameras offer high-resolution images to calculate canopy characteristics, but they are highly sensitive to illumination variations that provide inferior results (Barbedo, 2019). Ultrasonic sensors can detect canopies and gaps between trees through the transmission and reception of sound waves towards the target trees and manipulate the control of nozzles (Escolà et al., 2013; Palleja and Landers, 2015; Tumbo et al., 2002), with significant reductions in off-target losses (Jeon and Zhu, 2012; Llorens et al., 2010). Ultrasonic sensors may not be affected by illumination variation, but low measurement resolution, limited penetration capability, high dependency on the tractor speed, signal interference among adjacent sensors, and weather conditions are the main limitations of these sensors (Colaço et al., 2018). Therefore, ultrasonic approaches may not be practical for real-time precision spraying.

The LiDAR sensors transmitting infrared laser beams through a lens towards the orchard trees can penetrate small gaps in vegetation canopies and provide a fast measurement of canopy architecture with high resolution, which is not affected by weather conditions (Berk et al., 2016). These sensors have been used to detect tree presence, canopy size, and leaf density in orchards, nurseries, and vineyards with stable and independent accuracy while taking three-dimensional measurements (Chen et al., 2012; Liu and Zhu, 2016). They have also been successfully integrated into variable-rate precision sprayers tested in real-time field conditions, which resulted in uniform spray distribution with higher efficacy and efficiency (Boatwright et al., 2020; Cai et al., 2019; Chen et al., 2012).

Canopy density is an important measurement that can characterize tree structure and determine the appropriate spray volume for precise agrochemical applications (Hu and Whitty, 2019; Mahmud et al., 2021a; Wei and Salyani, 2005). Several studies have been conducted using LiDAR sensors, which showed high precision for tree canopy density measurements. Hu and Whitty (2019) used a mobile terrestrial system with 2D LiDAR to measure the canopy density distribution of a trellis structure and standalone apple orchards. The average correlation coefficient of the canopy density measurement was about 0.90. Mahmud et al. (2021a) measured the tree canopy density using a 3D LiDAR in high and low-density orchards and achieved a high correlation of 0.95 in low-density orchards compared to 0.82 in high-density orchards. Berk et al. (2020) calculated leaf area density using a 3D LiDAR and obtained a maximum correlation of 0.80 when establishing the relationship between tree canopy volume and leaf area density. Béland and Kobayashi (2021) reported the potential of using a multi-view terrestrial LiDAR sensor to map forest leaf area density even in dense tree areas. Mahmud et al. (2021b) used a 3D LiDAR-guided sensor fusion approach for tree canopy density correction considering uneven terrain conditions and reported a possible off-target spray reduction of 15.45%.

The primary component of airblast sprayers is a single fan that discharges airflow to carry spray droplets into target trees (Fox et al., 2008). The fan is driven by the tractor power take-off (PTO) located at the rear of the machine. For precision spray applications, appropriate spray deposition and coverage require that the volume of air released from the fan must be matched with the tree canopy density. Droplets can easily pass through the canopy if the airflow is too strong or cannot penetrate into the canopy if the airflow is too weak. Currently, sprayers typically discharge constant airflows that are independent of the tree canopy density. In most cases, the airflows are either too high or too low, resulting in either over- or under-sprayed crops (Zhu et al., 2008). Another major problem is that the fixed air velocity profiles can cause off-target deposition to air and ground (Gu et al., 2014; Zhu et al., 2006). Although significant amounts of research have been conducted on nozzle flowrate control (Khodabakhshian and Javadpour, 2021; Partel et al., 2021; Seol et al., 2022), very few studies have investigated automatic airflow control for orchard sprayers, particularly in real-time. Pai et al. (2009) designed and placed a deflector plate at the air outlet to control the airflow during spray operation, but the limited space at the air outlet hindered their system. A Cornell University engineer developed a circular airflow reducer (lately called the Cornell "doughnut") mounted on the fan inlet of orchard sprayers back in the 1980s. This method has been evaluated by European and American researchers to manually control airflow to improve spray application efficiency for orchard and vineyard sprayers. Marucco et al. (2008) developed a manually adjusted airflow velocity adjustment system for air blast sprayers and evaluated the spray deposition by considering the different airflow velocities and sprayer forward speeds. Their study focused on adjusting the airflow velocity based on the sprayer's forward speed instead of using the canopy density information of trees. Gu et al. (2012) installed an iris damper at the air inlet (rear of the sprayer) to manually regulate air velocities and later attempted to vary the airflow rates by changing the fan inlet diameter, considering different sized trees and canopy densities (Gu et al., 2014). Both experiments were conducted in laboratory conditions with fewer trees, which is usually different from field conditions. The literature review indicates that most previous research efforts were unable to automatically control the airflow in field conditions, which is needed for successful spray coverage on targets with reduced off-target loss.

The primary goal of this research was to develop an automatic control system for precision orchard sprayers to regulate airflow based on canopy foliage density in real time. The automatic control was achieved by manipulating the air inlet

diameters using an iris damper to simultaneously match the foliage density measurements using a LiDAR sensor under field conditions. The specific objectives were to (1) investigate the airflow penetrations on different tree densities with five different damper openings; (2) evaluate the spray coverage on different tree densities with different damper openings; (3) establish relationships between tree canopy points and airflow penetration, and tree canopy points and damper openings; and (4) evaluate the performance of the automatic system in orchard conditions.

Materials and Methods

Integration of the Airflow Control System

An automatic airflow control system was developed by integrating a 3D LiDAR range sensor, a micro-controller, a stepper motor, and an iris damper into an existing intelligent sprayer (fig. 1a). The three-point hitch-mounted airblast intelligent sprayer (Smartguide Systems Inc., Indianapolis, IN, USA) was used as a base unit. This was a standard PTO-powered sprayer (Pak Blast 150, Rear's Manufacturing Co., Coburg, OR, USA) equipped with a 2D LiDAR scanner, sixteen hollow cone nozzles (eight per side) coupled with solenoid valves, a 567 L (150 gallon) tank, a PTO-driven axial-flow fan (30 inches (0.76 m) diameter; 32° blade pitch), and a tablet computer (Samsung Electronics Co. Ltd., Suwon-Si, South Korea). The axial-flow fan had two operating speeds (540 and 1000 rpm). The 1000 rpm speed was used since some dense tree canopies were involved in the study. The air outlet of the sprayer was formed with an inverted U-shaped slot of 1.44 × 0.13 m on each side along its periphery. Under the standard fan setting, the total calculated volume rate of air output was about 16 $m^3 \cdot s^{-1}$.

The 3D LiDAR range sensor (Model# VLP-16, Velodyne LiDAR, San Jose, CA, USA) was mounted at the center of the sprayer unit with an aluminum frame at 1.9 m above ground level. It had the ability to scan up to 0.3 million points per second with an accuracy of ±3 cm. Tree canopies were scanned by the 3D LiDAR sensor, and the scanned information was saved on a laptop computer (Dell Technologies Inc, Round Rock, TX, USA) which was placed on the tractor unit. The scanner produced 16 vertically separated beams (eight at the left and eight at the right) with an angular resolution of 2° to scan the fruit trees (Mahmud et al., 2021a).

The iris damper (Continental Fan Manufacturing Inc., Buffalo, NY, USA) was retrofitted to the sprayer air inlet for airflow control (fig. 1a). It consisted of a casing, damper blades, and a regulator. The internal and external diameters of the iris damper were 0.80 m (31.4 in) and 0.81 m (32 in) (fig. 1b). The iris damper adjusted air inlet openings to control outlet airflow based on tree canopy variability. A high torque planetary geared stepper motor (NEMA 17, OSM Technology Co. Ltd., Ningbo, China) was attached to the regulator of the iris damper to precisely control the air inlet opening. The motor had a 0.035° step angle with NEMA 17 bipolar 4-wire, a planetary gearbox ratio of 50:9:1, a rated current of 1.68 A, and a resistance of 1.65 ohms. An Arduino Mega 2560 microcontroller board (Arduino LLC, Somerville, MA, USA) controlled the airflow regulator through the step motor to adjust the air inlet openings.

Airflow Control Model Development

Canopy Density Measurement

To determine the canopy density variability of the trees, the number of canopy points of individual trees was calculated based on data collected from the scanner. Data were collected from three different sized trees in three different orchard sites. The first site was planted with GoldRush cultivar (trees with medium canopy density, planted in 2009, trained as tall spindle, BBCH: 75), the second site with Gala cultivar (trees with high canopy density, planted in 2002, trained as tall spindle, and BBCH: 75), and the third site with Fuji cultivar (trees with low canopy density, planted in 2016, trained as tall spindle, BBCH: 75). The orchard sites were located at the Penn State Fruit Research and Extension Center, Biglerville, Pennsylvania, USA. Five trees from each site were studied, which provided a sufficient number because the variation of tree canopies within an orchard block was not high. Trees were randomly picked from different rows to cover the entire experimental plot. The trees were classified as low, medium, and high densities based on the number of canopy points scanned by the LiDAR scanner. The trees were scanned from a constant height (1.9 m above ground level) regardless of tree size. Trees randomly selected from

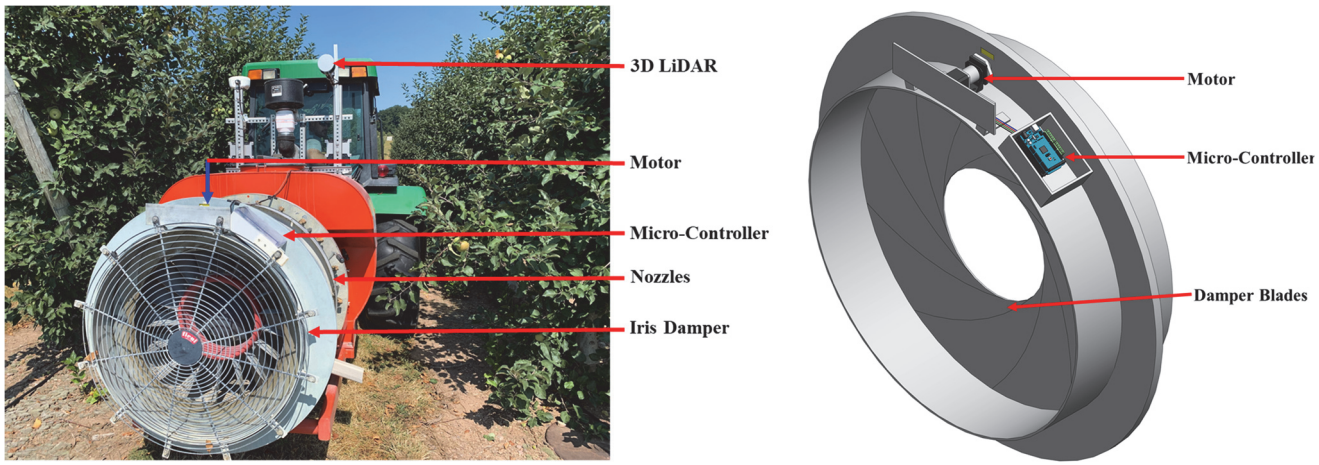

Figure 1. Automatic airflow control system mounted on LiDAR-guided orchard sprayer: (a) hardware integration and (b) iris damper.

three rows (two trees from the first two rows and one from the third row) were scanned from each site. A LiDAR data acquisition program was developed in MATLAB® (The MathWorks Inc., Natick, MA, USA) to scan the trees. To receive point cloud data from the scanner, a default User Datagram Protocol (UDP) port value of 2368 was used. A custom *velodynelidar()* function was used to initiate the tree scanning. The frame size in the x, y, and z-axis directions was defined before data collection (tree scanning). A *start()* function began the data acquisition. The acquired data were stored on the laptop computer for future calculation of the number of canopy points from the scanned trees.

The tree canopy density measurement procedure described by Mahmud et al. (2021a) was employed to calculate canopy point density for 15 scanned trees from the three sites. Each scanned tree included point cloud data that represented the geometric coordinates of tree canopies. Point cloud data were transformed to render the canopy points straight like the original orientation of the trees. The point cloud data that represented points from the ground and other sources (including trees from the same and different rows) were removed during pre-processing. Only the canopy points from the experimental trees were segmented by setting the region of interest (ROI). The ROI was different among the three cultivars due to different tree heights and widths. An ROI of -0.5 to 0.5 m in the x-axis, -3 to -1 m in the y-axis, and -2 to 2.5 m in the z-axis were used for GoldRush and Gala trees with medium and high densities, respectively. Although the plant spacing was different among these two varieties, the ROI used in the x-axis direction was the same because the canopy width of the two cultivars was the same. Due to the larger plant-to-plant distance, there were gaps between GoldRush trees, whereas the Gala site had a narrower plant-to-plant distance; therefore, trees were highly dense. An ROI of -0.4 to 0.4 m in the x-axis, -3 to -1 m in the y-axis, and -1.5 to 1.5 m in the z-axis were used for Fuji trees with low density. Individual ROI canopy points were counted using the custom *findPointsInROI()* and *select()* functions. The first function was applied to find the canopy indices, and the second function was applied to count the number of ROI canopy points. The total number of counted points was used to assess the density of targeted trees (fig. 2).

Airflow Measurement

To determine the effective airflow required for trees of a particular density, the airflow was measured and spray operations were performed with different iris damper air inlet openings. Five different openings were investigated: opening 1, opening 2, opening 3, opening 4, and opening 5, with opening diameters of 0.80 m (31.4 in), 0.69 m (26.97 in), 0.57 m (22.62 in), 0.46 m (18.27 in), and 0.34 m (13.3 in), respectively (figs. 3a to 3e). The maximum and minimum opening diameters of the damper were 0.80 m and 0.34 m.

Airflow was measured at the backside of the trees about 0.64 m from the tree trunk with all the damper openings one at a time. The 0.64 m distance was chosen because this was the distance from the edge of the trees at the backside to the trunk (fig. 3f). A handheld Kestrel 3550AG weather meter (Kestrel Instruments, Boothwyn, PA, USA) at a constant height of 1.55 m measured the airflow. The constant height was used to maintain the uniformity of the data collection. One airflow reading was recorded from one damper opening under the same wind condition (low wind). A total of five airflow readings were recorded from one experimental tree. The maximum airflows were recorded. All experiments were conducted at the end of June 2021 during low wind conditions with wind speeds between 0 and 1.5 $km \cdot h^{-1}$.

Spray Coverage Measurement

The spray operation was conducted five times on each tree with the five damper openings. The spray operation was accomplished using the intelligent sprayer with one damper opening at a time in each targeted tree. The spray volume discharged from the sprayer was automatically controlled by the tree canopy density. Water sensitive papers (WSP) (Syngenta Crop Protection AG, Basel, Switzerland) with a size

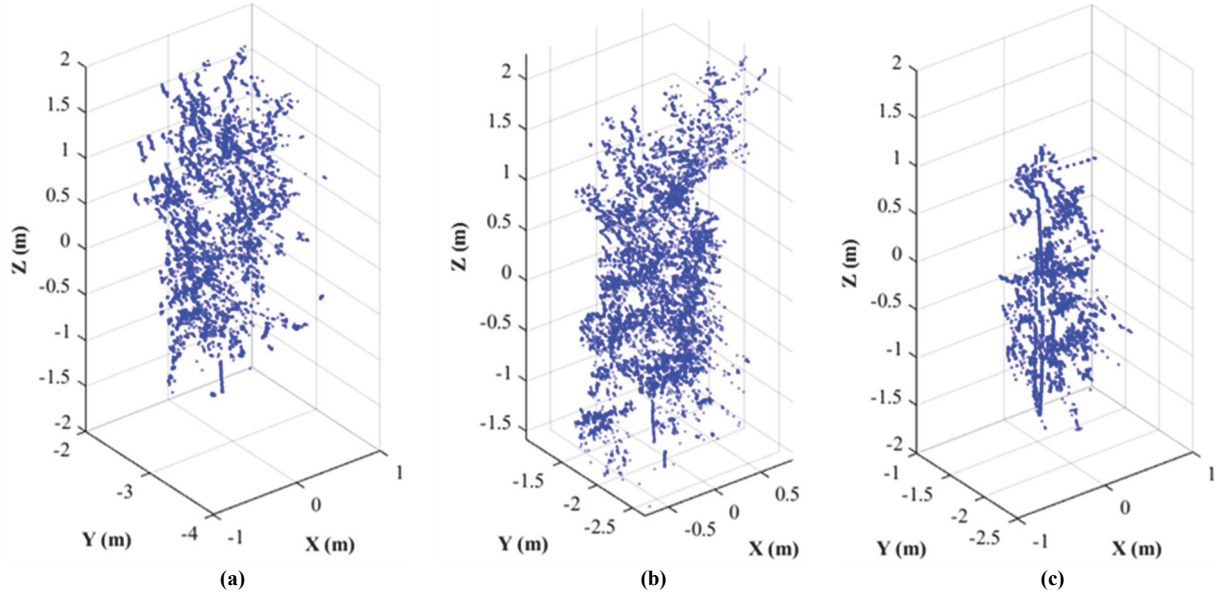

Figure 2. Scanned apple trees from three orchard sites (a) canopy points from GoldRush cultivar tree, (b) canopy points from Gala cultivar tree, and (c) canopy points from Fuji cultivar tree.

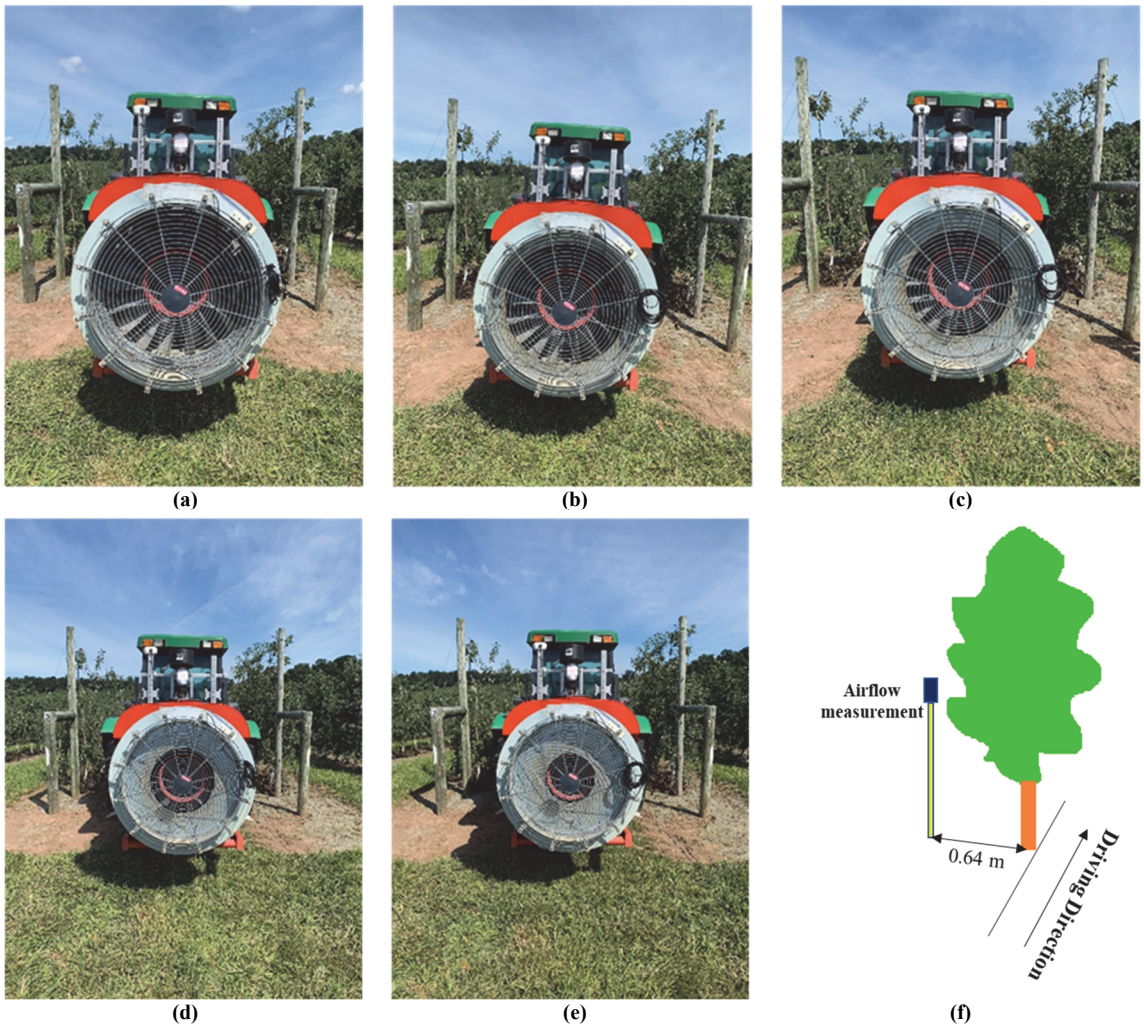

Figure 3. Five different damper openings were used for study (a) opening 1 (0.8 m dia), (b) opening 2 (0.69 m dia), (c) opening 3 (0.57 m), (d) opening 4 (0.46 m dia), (e) opening 5 (0.34 m dia), and (f) experimental setup of anemometer at height of 1.55 m for airflow measurements.

of 26 mm × 76 mm were used to measure spray coverage as a spray deposition indicator to validate the airflow control system. They were placed at twelve different locations on the tree before each spray operation (fig. 4). The twelve locations were three at the ground (L1, L2, and L3), bottom (L4), middle (L5), top (L6), two at the backside at the same height of L5 parallel to the driving direction (back-left and back right when facing toward the tree) of the tree (L7 and L8), and four at the edge of the next tree row (L9, L10, L11, and L12). Coverage uniformity was assessed using the WSPs because of their simplicity of visualization (Salyani and Fox, 1999; Cerruto et al., 2019) (fig. 5). The papers were collected after drying and stored in sealed bags until they were analyzed. After collecting WSPs for one spray operation with one damper opening, the new WSPs were placed for the second damper opening for the next spray operation. The WSPs were placed for five rounds for each tree, for a total of five damper openings. The WSPs were scanned in the laboratory using a portable business card scanner (CSSN Inc., Los Angeles, CA, USA) with imaging resolution at 600 dpi and a scan capability width of up to 10.5 cm. The spray coverage on each WSP was assessed using the DepositScan program (Zhu et al., 2011).

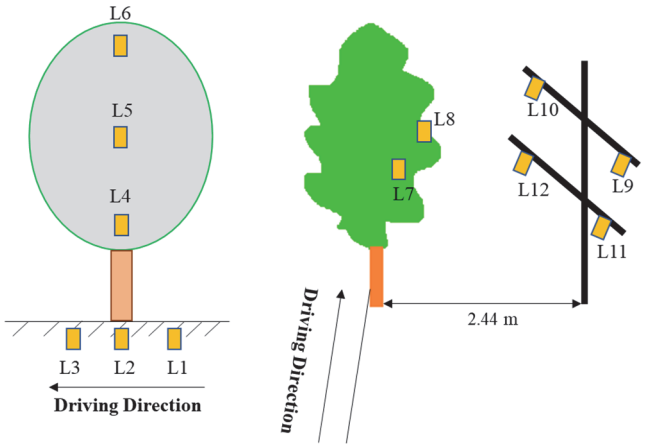

Figure 4. Experimental setup for spray coverage test with water-sensitive papers placed (marked as orange rectangle) at twelve different locations (L1 to L12) (L1, L2, L3 on ground, L4 at 0.8 m, L5 at 1.6 m, L6 at 2.4 m, L7 & L8 at 1.8 m, L9 & L10 at 2.2 m, L11 & L12 at 1.4 m).

Model Development

The iris damper had a damper position adjustment nut, allowing different openings with different angular inputs. The relationship between the stepper motor steps and the

(a) (b)

Figure 5. Water sensitive paper placed in tree (a) before and (b) after spray operation.

openings of the iris damper was established (fig. 6). This model was used for the motor step input for later studies in both airflow control model development and field validation of the developed airflow control system.

The relationship between the canopy point densities and recorded airflows from the five different damper openings was established. The appropriate damper opening for the trees was selected based on counting the highest number of WSPs with uniform spray coverage among the five openings. The uniformity of coverage was computed by dividing the mean coverage by the 20th percentile coverage. The airflow was chosen from the damper opening and was proven effective for the particular tested tree. For example, the sprayer with a damper opening of 0.69 m (26.97 in) diameter and corresponding airflow of 8.5 km·h^{-1} resulted in a total of eleven (out of twelve) WSPs with uniform spray coverage on tested tree no. 4 (canopy point density of 13,000), higher than other openings. The opening of 0.69 m and airflow of 8.5 km·h^{-1} were then chosen for that type of tree. A similar procedure was followed for all the trees. Based on the evaluation of spray coverage on WSPs, three damper openings were chosen for three sites with low, medium, and high-density trees. The recorded canopy points of trees and their effective damper openings were used to develop a mathematical model to predict the required damper opening and airflow for any sized tree. The corresponding airflows from the selected three damper openings and canopy points were used to develop a mathematical model for predicting inlet airflow with canopy point changes.

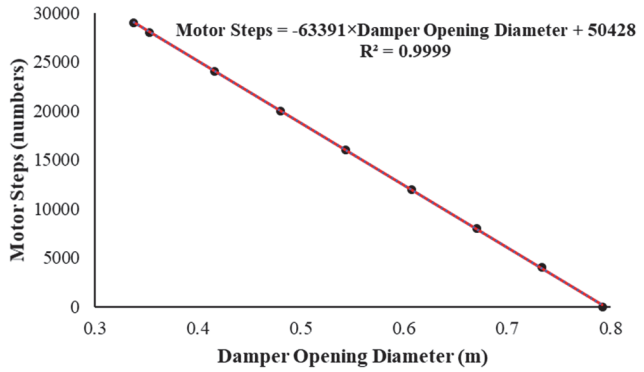

Figure 6. Relationship between damper opening diameter and motor steps.

Algorithm for Automatic Damper Control

An algorithm was developed to adjust the damper opening based on tree canopy points to provide appropriate airflow for adequate spray coverage on the tree. Figure 7 shows the workflow diagram of the algorithm. Figure A1 shows the pseudo-code of the algorithm written with MATLAB®. The algorithm initialized the 3D LiDAR sensor that was used to scan the trees. The Arduino port was opened to build a serial communication between the computer and the micro-controller. The initial damper position was set to zero at the beginning. The zero position meant the damper was at its maximum opening of 0.80 m in diameter. The *readframe()* function read frames from the LiDAR sensors. The frames were processed one after another using a loop. The frames captured the scanned point clouds of the trees. Each frame was oriented differently from the original tree; therefore, the transformation was performed to make the shape of point clouds similar to the scanned tree. The transformation consisted of two steps at the defined coordinate using transformation equations 1 and 2. First, each coordinate of tree point clouds was oriented at 90° counter-clockwise around the z-axis, and second, the resulting coordinate was rotated 90° clockwise around the y-axis.

Counter-clockwise rotation (90°) around z-axis

$$R_z\left(\gamma = 90^\circ\right) = \begin{bmatrix} cos\,\gamma & -sin\,\gamma & 0 & 0 \\ \sin\gamma & \cos\gamma & 0 & 0 \\ 0 & 0 & 1 & 0 \\ 0 & 0 & 0 & 1 \end{bmatrix} \quad (1)$$

Clockwise rotation (90°) around the y-axis

$$R_y\left(\beta = 90^\circ\right) = \begin{bmatrix} cos\,\beta & 0 & -sin\,\beta & 0 \\ 0 & 1 & 0 & 0 \\ sin\,\beta & 0 & cos\,\beta & 0 \\ 0 & 0 & 0 & 1 \end{bmatrix} \quad (2)$$

The transformed tree point clouds had points from the ground and points from other trees located in the same and other rows. The ROI extracted points from the targeted tree based on the average tree width, height, and canopy depth of the corresponding sites (GoldRush and Gala). The ROI of -0.62 to 0.62 m in the x-axis, -3 to -1 m in the y-axis, and -2 to 3 m in the z-axis were used. The same ROI was used for all sites due to their same tree canopy width. To remove the ground points, the M-estimator SAmple Consensus (MSAC) algorithm was used, which is a variant of the Random Sample Consensus (RANSAC) algorithm (Torr and Zisserman, 2000). This algorithm found the outlier points from the acquired point clouds. The outlier points were removed to obtain only the tree canopy points (without ground points). To count the tree canopy points of each tree, the number of indices within the ROI was calculated using *findPointsInROI(), select(), and indices.count()* functions. The LiDAR frames also covered the open area between trees and partial trees. The algorithm set the threshold value for

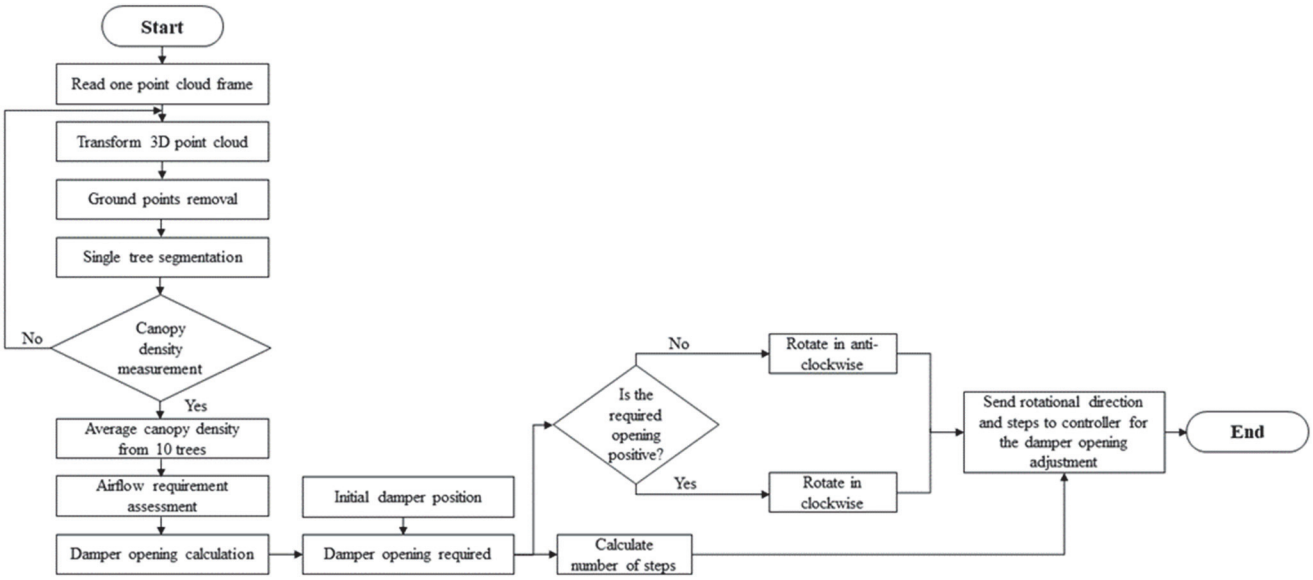

Figure 7. Workflow diagram of algorithm developed for automatic damper control scripted in MATLAB®.

the orchard sites to avoid these frames for the damper control. A minimum threshold of 5,000 canopy points for medium-density trees (GoldRush) and 10,000 for high-density trees (Gala) was used. The threshold value was computed from the calculated minimum canopy points in a tree from each of the respective sites (based on section 2.1.3: tree canopy points density measurements). The algorithm skipped five frames after completing one iteration. For example, if it processed frame number one, then the next process frame number would be seven. The number of frames to be skipped was calculated based on the average canopy width of each site, the LiDAR frame rate, and the ground speed of the sprayer. The tree canopy width was about 1.24 m, the LiDAR frame rate was five frames per second, and the sprayer ground speed was about 1 $m \cdot s^{-1}$ (3.6 $km \cdot h^{-1}$). The five frames from the LiDAR could have the same information from the same tree; therefore, one frame was sufficient to process one tree and avoid overlap based on the canopy width and sprayer speed.

The mechanical motion of the damper regulator took about three seconds to move from maximum opening to minimum opening, which limited the system control speed for responding to individual tree canopy densities. Therefore, average canopy densities were used instead of the canopy point density of a single tree to control the damper because the LiDAR scanner speed was faster than the damper adjustment speed for the required opening. Another reason was that trees that grew in the same row or even in the same orchard block could have relatively uniform canopy density. Therefore, adjusting/controlling the damper opening based on the average density of a few trees should be acceptable for spraying trees in the same row or the same orchard block. Average canopy density was computed for damper control before spraying. The algorithm captured and then averaged the canopy point densities from ten trees in a row (fig. 8). The average canopy density was used to calculate the required damper opening and motor steps using the two models from the previous section. The motor steps and direction

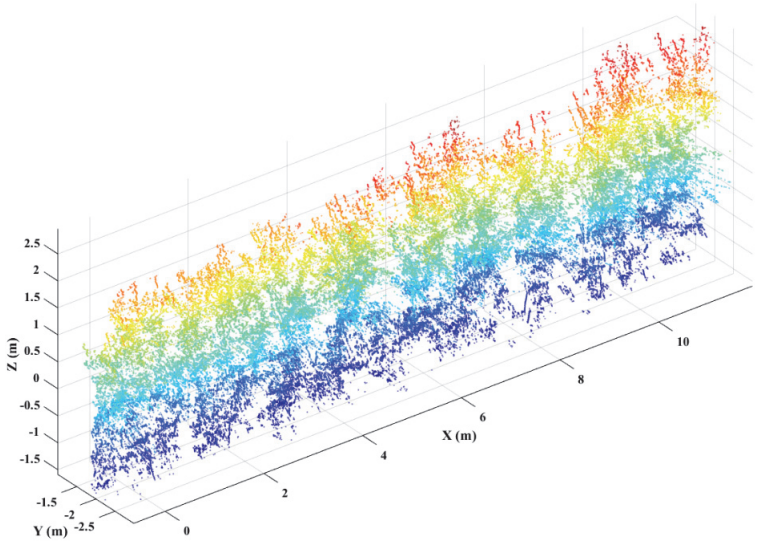

Figure 8. Canopy points scanned from ten consecutive trees of tested orchard site (Gala). Different colors represent Z value (height) of point cloud.

(clockwise) were sent to the microcontroller through serial communication. The motor rotational direction was clockwise (+ve) because the initial position of the damper was set to full open. A stepper motor control program was uploaded to the Arduino to receive steps and rotation information to control the damper openings for automatic airflow control during the spraying operation.

Field Validation of Developed Airflow Control System

Field tests were conducted on calm days (low wind conditions) to evaluate the performance of the automatic airflow control system. As stated in the algorithm development section 2.3, the airflow control system was tested in two orchard sites: GoldRush orchard with medium density and Gala orchard with high density. These two orchards were the same sites where the initial experiments were conducted, but the field tests were performed with different rows and trees 1.5 months later. The row spacing was 2.66 m. The plant spacing in a row was 1.68 and 1.24 m for GoldRush and Gala, respectively. However, average tree canopy widths in both sites were the same (about 1.24 m ± 0.3 m).

Figure 9 illustrates the experimental setup for the airflow control system field validation. Five trees were randomly selected from three rows in each site. Two types of tests were conducted: controlling the damper opening based on individual tree canopy point density and controlling the damper opening based on the average tree canopy point density from ten consecutive trees in a row. The damper control based on an individual tree was tested to compare the actual airflow generated by the system at the back of the tree with calculated or theoretical airflow based on the airflow model.

Two airflow models were used for two test sites. The models were $airflow = 2047.2 \times canopy\ points^{-0.65}$ and $airflow = 2535.9 \times canopy\ points^{-0.653}$ for GoldRush and Gala, respectively. These two models were chosen from five relationships using five damper openings. The models were selected based on the average tree canopy points of each site and their required damper openings. For example, the average canopy point of the GoldRush site was 9,566, and therefore the calculated required damper opening was 0.59 m. Based on the airflow models from five damper openings, the model developed with damper opening 3 (an opening with a diameter of ~0.57 m) was very close to the required opening. Therefore, the airflow speed model with opening 3 was used for the theoretical airflow calculation for the GoldRush site. A similar procedure was followed for the Gala site, where an airflow speed model with opening 2 was used.

The algorithm developed in section 2.1.5 was used for experimental airflow measurements, and the loop iteration was set to one because one frame was used to calculate canopy points and the required damper opening for a target tree. Airflows were measured at the back of the tree after the required damper opening was reached. The number of canopy points and measured airflow were recorded for analysis. The average canopy points density was also calculated using the same algorithm, but the loop iteration was set to 10 (i = 1:55; skipping five frames). The average canopy point density was computed to observe the tree canopy variability within a row. Three average canopy point densities from three rows were calculated to adjust the damper opening separately for each row. Based on the average canopy point density in each row, the damper opening and spray operations were performed on targeted trees. The WSPs were placed at 12 locations (same as initial experiments) for evaluating spray coverage. A similar procedure was followed for the WSP collection after spray operation and analysis.

Statistical Analysis

One-way Analysis of Variance (ANOVA) along with Tukey's test determined the difference of spray deposits among five different openings using Minitab® 19 statistical software (Minitab® Inc., State College, PA, USA). The coefficient of determination (R^2) was calculated between tree canopy points and airflows for performance evaluation. A Duncan post-hoc test was performed after a one-way ANOVA to evaluate the difference of spray deposits among six sections of the tested orchard sites.

Results and Discussion

Air Penetrations at Various Density Trees

Figure 10 shows the maximum airflows recorded at the backside of the test trees from three sites with five different openings. The sprayer ground speed was 3.6 km·h^{-1}. Overall, air penetration through canopies was higher in the lower-density trees compared to the medium and higher-density trees. As the tree canopy points increased, the air penetration

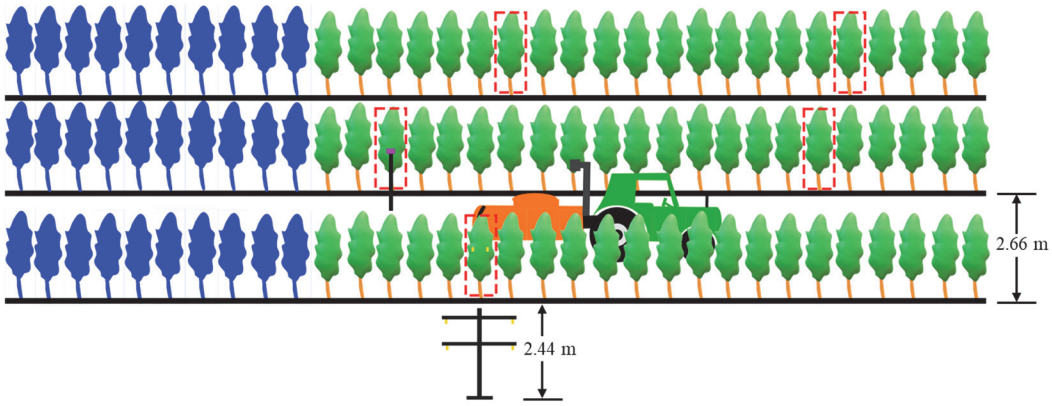

Figure 9. Experimental setup for validating airflow control system (blue trees represent scanned trees to control damper for spray operation, and red box represents targeted trees).

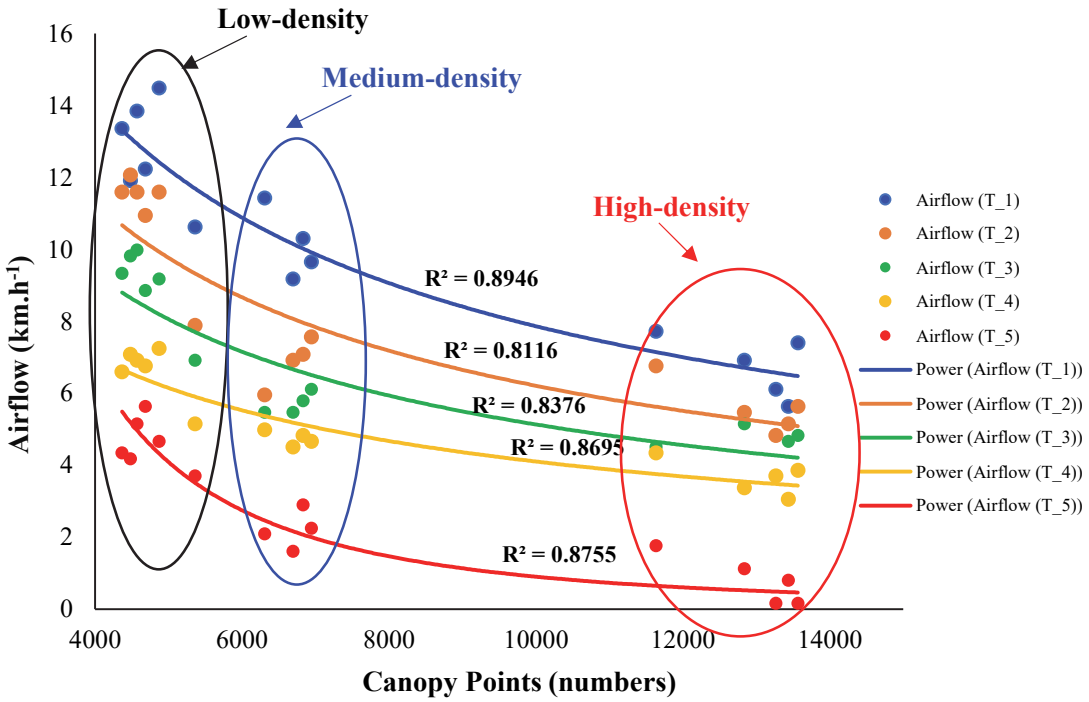

Figure 10. Relationship between tree canopy points and airflows from five damper openings.

through the canopies decreased. The high-density trees normally had more canopy points that could substantially block the air from passing through the canopy to reach the anemometer. This implies that the high-density trees require a high airflow to transport droplets through the canopies, while the lower airflow should be sufficient for low-density trees. These results agreed with Pai et al. (2009), who highlighted the necessity of airflow control due to canopy variations. The recorded airflows from the damper openings showed good correlations with the number of tree canopy points. The R^2 values of the "airflow-canopy relationship" were 89.5%, 81.2%, 83.8%, 86.9%, and 87.6% for openings 1, 2, 3, 4, and 5, respectively. The small difference between the R^2 values using different openings might be due to a slight variation of wind at the specific locations of the experimental sites.

Although all the damper openings provided strong correlations, the recorded airflows were different. In general, the airflow at the backside of the tree increased as the damper opening increased. With the larger damper opening, relatively more air entered the fan chamber, which released more air from the outlet. Higher airflow could result in higher movement of the spray droplets beyond the tree canopy. The movement of the spray droplets with the same airflow could be different depending on tree canopy densities. This implies the importance of tree canopy density measurement for sprayer airflow control. Although strong correlations were achieved from all damper openings, the spray droplet coverage could be different due to variations in canopy densities. The droplet coverage is an indicator of sprayer performance, showing spray operation quality to provide adequate disease and pest control. Therefore, it is important to identify which opening is suitable for which type of tree based on the evaluation of spray coverage.

It is worth noting that the ambient wind speeds minimally affected these experiments because they were conducted at low wind conditions (wind speeds between 0 and 1.5 km·h^{-1}) as recorded by the nearby weather station. Also, the airflows were measured at the lower height of 1.55 m from the backside of the tree, which could have had a negligible effect from the low-speed wind. Measurements were taken at a fixed distance from the tree trunk to ensure consistency.

Spray Coverage on Various Density Trees in Three Orchard Sites

As shown in figure 11, spray coverages were significantly affected by the damper openings at the 95.0% confidence level. Spray deposits at the ground, top, middle, bottom, backside, and next row were compared separately among five damper openings. The sprayer discharged the same amount of spray volume for a targeted tree for all five openings. Variations of the spray deposits were observed due to the change of the airflows (from different damper openings). A particular damper opening is considered good if it showed higher coverage on tree canopy sections (top, middle, bottom, and backside), and lower coverage at off-target sections (ground and next row), would be chosen for those types of trees. Overall, damper openings 1, 2, and 5 provided significantly lower mean coverages at tree sections than opening 3 and 4 in most cases. At openings 1 and 2, a portion of the spray droplets mostly discharged from the upper nozzles drifted to the open air and other rows before reaching the target trees, perhaps due to the high airflow. This resulted in higher coverages in the next row of the orchard, which were significant among other openings. This situation was also confirmed by visually observing WSPs on targets. For opening 5, a portion of droplets was deposited to the ground, mostly from the lower nozzles. In other openings, mean coverages were 45.9%, 49.9%, 57.6%, 37.2% (opening 3), and

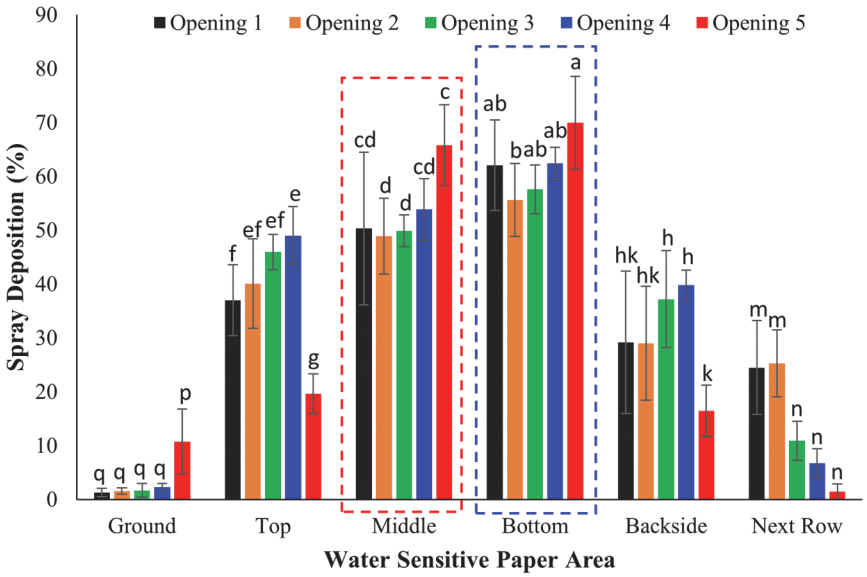

Figure 11. Spray coverages at six different sections for GoldRush orchard (medium density). Groups identified by same letter did not differ statistically. Average spray coverage on different sections from five experimental trees is shown. Two boxes are presented as examples to illustrate statistical comparisons of spray coverages between five openings for each section, where comparisons for each section are independent of each other.

49.0%, 53.9%, 62.4%, and 39.8% (opening 4) at the top, middle, bottom, and backside, respectively. The off-target coverages at the ground and next row were also lower. This might be due to the match of the airflow profile required for adequate spray coverage on these types of trees. The results showed no significant difference between openings 3 and 4 for spray coverage at the bottom and backside, but the spray coverages were significantly higher at the top and middle sections for opening 4 compared to opening 3. Therefore, opening 4 was chosen for these types of trees (average height and canopy points were 3.6 m and 6242, respectively) for spray operations.

Spray coverage results for the Gala orchard (with high-density trees) using five different openings are presented in figure 12. The spray coverages at the middle and bottom sections showed no significant difference among the five damper openings; however, there were significant differences in droplet coverages for the top and backside. The density of tree canopies was higher in the middle and lower sections, blocking the majority of the spray droplets. For the top and backside sections, the sprayer did not generate enough airflow using openings 3, 4, and 5; thus, it could not deliver enough droplets to those sections with these three openings. Using openings 1 and 2, the spray coverages for those sections were relatively higher, but they were not significantly different. However, fewer droplets drifted to the next row with opening 2 compared to opening 1. On the ground, openings 1 through 4 produced lower spray coverage than

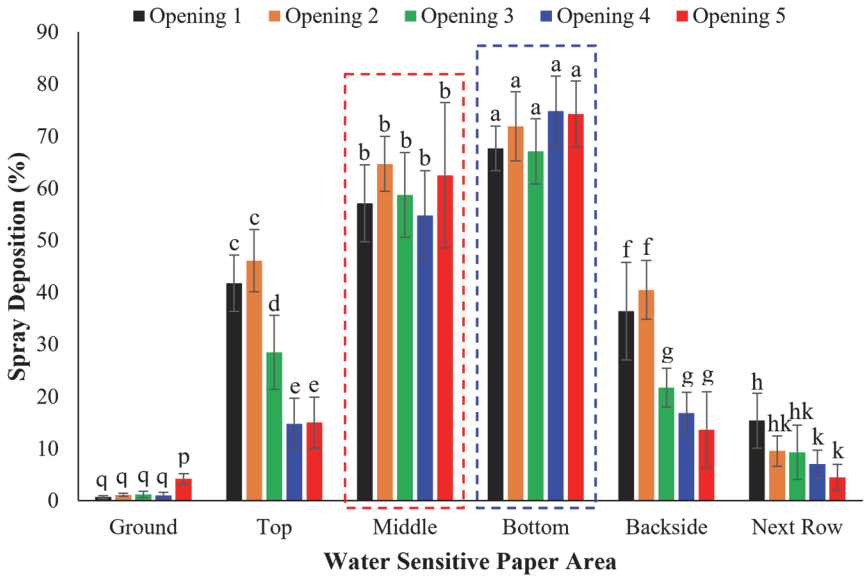

Figure 12. Spray coverages at six different sections for Gala orchard (high density). Groups identified by same letter did not differ statistically. Average spray coverage on different sections from five experimental trees is shown. Two boxes are presented as examples to illustrate statistical comparisons of spray coverages between five openings for each section, where comparisons for each section are independent of each other.

opening 5. Based on the spray coverage quantities at all sections, opening 2 was selected for these types of trees (average height and canopy points were 3.8 m and 12836, respectively).

Figure 13 shows the results of spray coverage using five damper openings in the Fuji orchard with low-density trees. Similar to the Gala orchard, the spray coverages at the middle and bottom tree sections showed no significant differences among all damper openings. Damper opening 5 provided greater coverages on all four tree sections than the other four openings. Some unexpected higher coverage results were observed with opening 1 than those with other openings, which might be due to increased ambient wind when opening 1 test was conducted. In comparison, the amount of spray deposits for opening 5 on downwind row trees was significantly lower than those with other openings, but the ground coverage was significantly higher. However, the mean ground spray coverage for opening 5 was about 5.35%, which was much lower than those in the four tree sections. Thus, opening 5 was chosen for low-density trees (average height and canopy points were 3.1 m and 5085, respectively).

Airflow Control Model

An airflow control model was developed based on the evaluation of spray coverages using different damper openings (fig. 14). The model shows strong prediction ability, with an R^2 of 97.5%. It offers automatic calculation of the required damper opening in response to the number of tree canopy points received from the LiDAR sensor. Although the model was capable of predicting the damper opening for any number of tree canopy points, the automatic airflow control system was programmed to adjust the damper opening within the range between 0.34 and 0.80 m (lower and upper limits of damper opening diameter). Ideally, another orchard block with tree canopy density in the range of 8,000 to 11,000 points could be selected for the test, but due to the limitation of resources, only three orchard blocks with densities ranging from high to low were used. With the three orchard blocks and 15 trees in total, it was sufficient to create the model to predict the damper opening based on the canopy density as shown in figure 14.

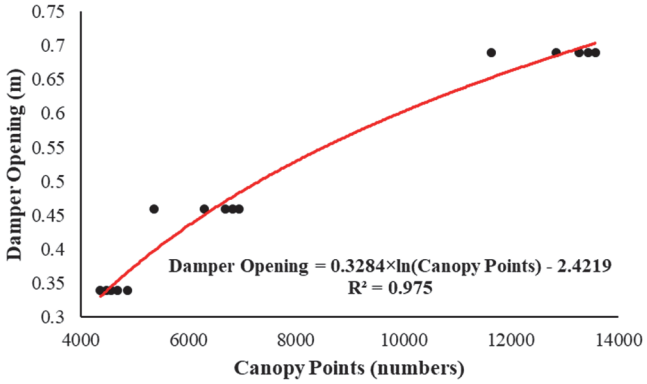

Figure 14. Relationship between tree canopy points density and required damper opening.

Field Validation

Comparison results from theoretical and experimental airflow measurements (table 1) reported a Mean Absolute Error (MAE) of 2.27 and 1.42 km·h^{-1} and a Root Mean Square Error (RMSE) of 2.41 and 1.6 km·h^{-1} for GoldRush and Gala orchards, respectively. The MAE and RMSE errors were lower in the high-density Gala orchard than in the medium-density GoldRush orchard. There were no gaps between trees in the Gala orchard, which provided smaller

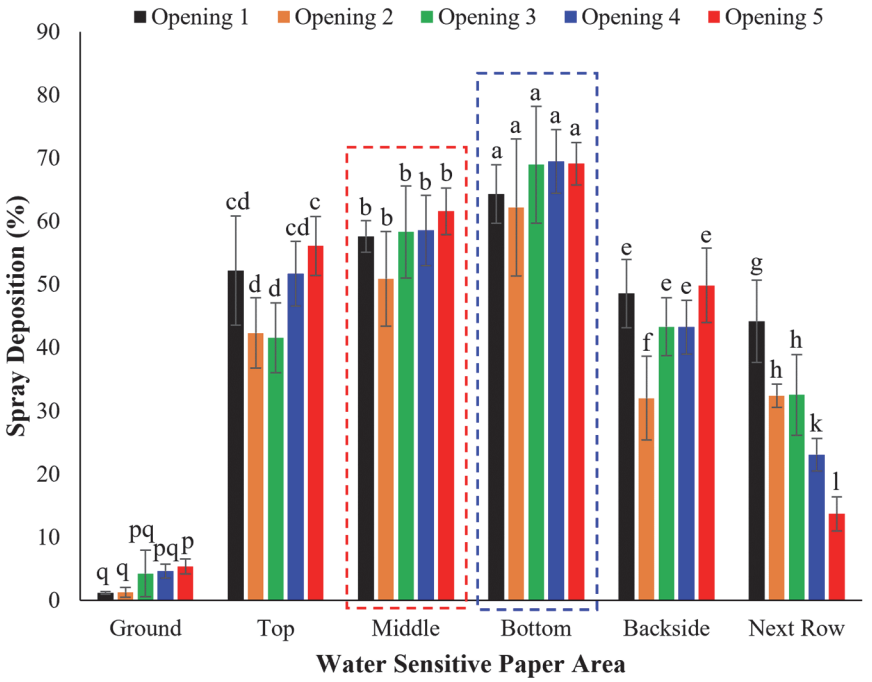

Figure 13. Spray coverages at six different sections for Fuji orchard (low density). Groups identified by same letter did not differ statistically. Average spray coverage on different sections from five experimental trees is shown. Two boxes are presented as examples to illustrate the statistical comparisons of spray coverages between the five openings for each section, where comparisons for each section are independent of each other.

Table 1. Comparison between theoretical and experimental airflow measurements during field tests.

Test Orchard	Tree No	Canopy Points	Theoretical Airflow (km·h^{-1})	Experimental Airflow (km·h^{-1})	MAE (km·h^{-1})	RMSE (km·h^{-1})
Orchard 1 (GoldRush)	1	10372	5.02	7.89	2.27	2.41
	2	9799	5.21	7.4		
	3	8530	5.7	6.92		
	4	10724	4.91	6.59		
	5	8404	5.76	9.17		
Orchard 2 (Gala)	1	12710	5.3	5.95	1.42	1.6
	2	14111	4.95	3.54		
	3	10291	6.08	8.72		
	4	15795	4.6	2.9		
	5	10735	5.92	6.63		

variations in measurements. Conversely, gaps between trees in the GoldRush orchard resulted in comparatively higher airflows than theoretical calculations because the air moved faster through the gaps. Tests in both orchards showed variations in the airflow measurements because of field variabilities.

The tree canopy variability within the same row and orchard block was evaluated by calculating the average canopy points from ten consecutive trees (scanned before reaching the target tree) and the individual target tree (table 2). The highest relative difference between average canopy points and individual tree points was 11.74%, which occurred in Row 1 of the GoldRush orchard. The canopy variability was comparatively higher in the GoldRush orchard than in the Gala orchard. This was because the trees in the GoldRush orchard were not trained adequately by modern tree training strategies. The Gala orchard was appropriately trained and showed low canopy variations among the trees in the row. This implies that the modern tree training strategy could substantially reduce the tree canopy variabilities of apple orchards. Furthermore, growers also prune trees to maintain low canopy variabilities in the same orchard in a growing season. These results indicate the potential for using one damper opening for a particular orchard block. However, the damper opening should be adjusted in different orchards with different tree sizes, ages, management practices, and cultivars. It is recommended to perform the spray operation during low wind conditions with no or minimal field variability.

The targeted trees were sprayed using the damper opening calculated from the average tree canopy points in an individual row. Since the canopy variations within a row were minimal, the average canopy points from the first scan of the row were used for the spray operation. This was also convenient because the damper opening was already adjusted. The amounts of spray coverage at six different sections were significantly different in two test sites (figs. 15 and 16). The bottom and middle sections received more spray droplets than the other sections in both sites. Overall, spray deposits at the top and backside sections were higher at the Gala site than at the GoldRush site. This was because the high-density Gala trees were able to block the major portion of air produced by the sprayer, resulting in high droplet coverage on those sections compared to the GoldRush orchard, where there were gaps between trees. The droplet coverage at the next row was also higher in this site than in the Gala site due to the gaps. However, ground coverages were small at both sites.

Table 2. Comparison between canopy points of the individual tree and ten consecutive trees from the same row.

Test Orchard	Tree Row	Canopy Points	Average Canopy Points of Ten Consecutive Trees	Relative Difference (%)
Orchard 1 (GoldRush)	Row 1	10372	9154	11.74
		9799	8891	9.27
	Row 2	8530	9312	9.17
		10724	9494	11.47
	Row 3	8404	8923	6.18
Orchard 2 (Gala)	Row 1	12710	11661	8.25
		14111	13149	6.82
	Row 2	10291	11189	8.73
		15795	14437	8.60
	Row 3	10735	11480	6.94

DISCUSSION

The major airflow attributes of airblast sprayers are their ability to agitate canopies and transmit spray droplets to the target tree sections. The requirement for airflow is different among trees and is primarily dependent upon tree canopy densities. High-density trees require relatively stronger airflow than medium-density trees, whereas relatively less airflow is required for low-density trees. However, identifying the airflow needed for particular canopy densities or orchard sites is challenging. Therefore, these results provide a potential approach for current precision airblast sprayers to match the airflow requirements of different canopy densities to reduce off-target spray coverages. Although this study was conducted with three types of tree canopy densities, the system is not limited to these. The damper opening control model can calculate the required opening for any canopy density. However, the damper opening has maximum and minimum limits, and cannot go beyond that limit when the calculated opening is out of the range. It should be noted that the airflow control system was developed with a specific configuration of the sensor, motor, micro-controller, sprayer ground speed, fan speed, nozzle type, and flow rate. Hence, it is very important to maintain the same configuration when integrating with the precision airblast sprayers.

Modern fruit trees planted in a row have low canopy density variation unless the trees are affected by severe diseases. This study reaffirmed that variation of the tree canopies within a row or even an orchard block was not high (maximum ~11.74%), which indicates the potential of a single damper setting for a row or an orchard block if they are the same variety and aged trees. The average canopy density of ten trees or even an entire row should be enough to identify the required effective airflow for a particular orchard block. Faster mechanical devices may make this system suitable for controlling airflow based on individual trees, although it is not critical due to lower canopy variation. The field validation results of our system provided improved droplet coverage within tree canopy sections and significantly reduced off-target coverage by controlling damper opening using average tree canopy points from ten consecutive trees. However, some tree sections showed lower spray coverage on WSPs due to field variabilities and uncertainties. For example, sometimes sprayer airflow pushed leaves over top of the WSP, resulting in lower spray coverage on the WSP

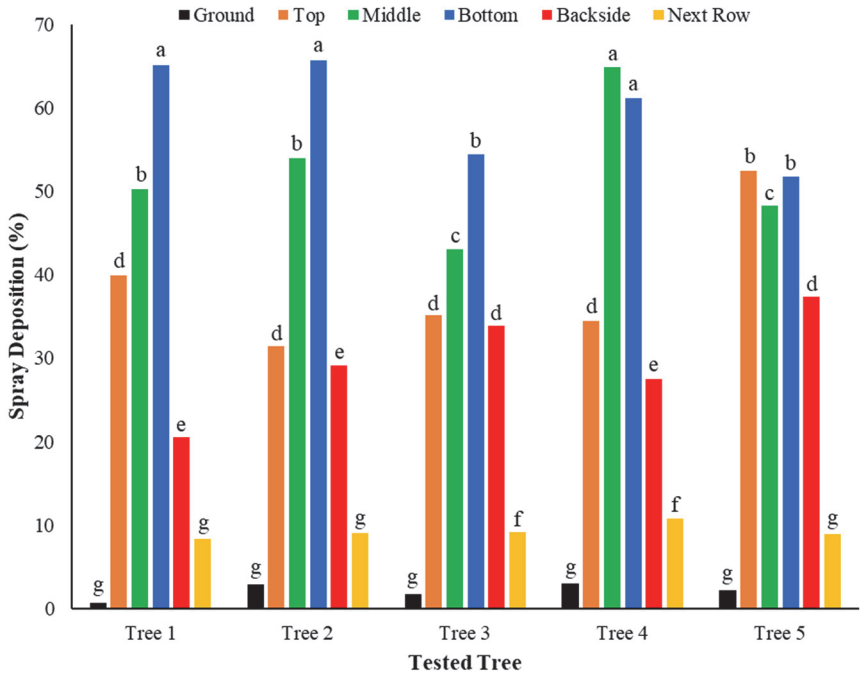

Figure 15. Spray coverage on five tested trees in GoldRush site (medium density) with opening 4. Letters represent homogeneous groups obtained by Duncan post-hoc test ($p \leq 0.05$). Groups identified by same letter did not differ statistically.

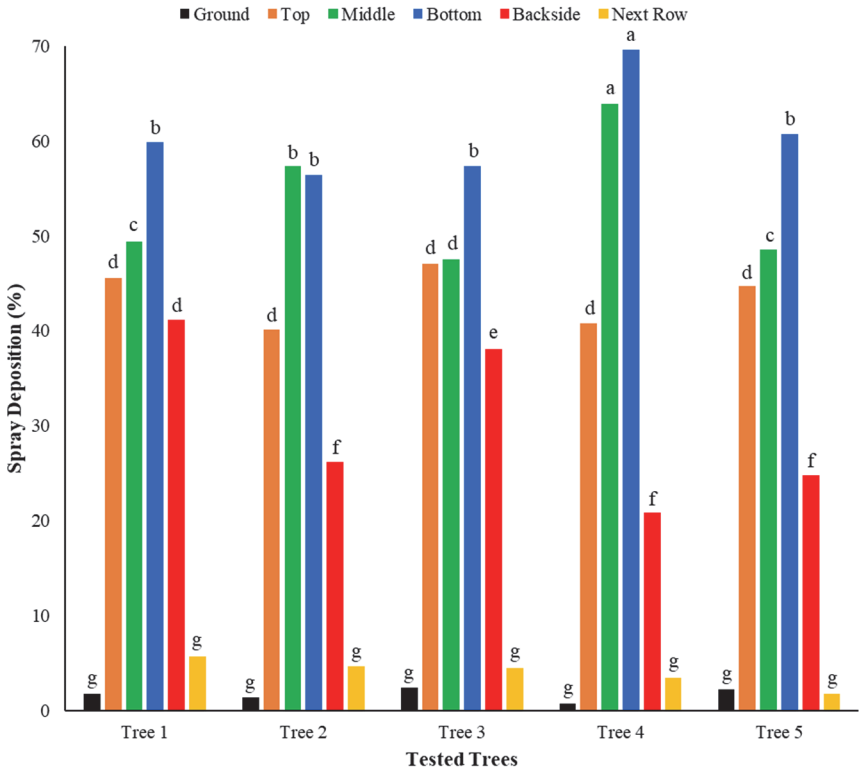

Figure 16. Spray coverage on five tested trees in Gala site (high density) with opening 2. Letters represent homogeneous groups obtained by Duncan post-hoc test ($p \leq 0.05$). Groups identified by same letter did not differ statistically.

(fig. 17). The position of the airflow measurements was also a cause of measurement error between theoretical and experimental airflows. Although the measurements were taken at a fixed distance and position from the tree trunks, the variability of canopy densities in front of the anemometer caused some deviation in airflow measurements, resulting in errors.

Overall, the experimental results reaffirmed that adjusting the fan air inlet could control airflow penetration into tree canopies and reduce off-target spray coverage and drift. Instead of adjusting airflow for individual trees, it is more realistic to control the damper opening based on the average tree canopy density of a row or an orchard block for variable-

Figure 17. Lower spray coverage at top portion of WSP due to leaf blockage.

rate spraying. The current system can be applied for practical use. The process of scanning trees and then adjusting opening sizes based on the average canopy density of 10 consecutive scanned apple trees was automatic. However, the control per tree requires a faster mechanical system and controller improvement. The average canopy densities need to be measured before the spray operation. One-time measurement of the average density should be sufficient for an orchard block with the same tree age, cultivar, and density. Continuation of this study with faster mechanical systems and advanced motors and controllers with different tree canopy densities could meet the needs for very precise airflow controls and could guide the development of the automatic airflow control system for real-time airflow adjustment and spray operation for individual trees.

Conclusions

An automatic airflow control system was developed to distribute adequate air to successfully carry droplets from the sprayer to the target trees by reducing off-target coverage and drift. The system consisted of an electro-mechanical controller which had the capability of changing air inlet diameter with an iris damper. Three different tree canopy densities (low, medium, and high) were studied, and results showed that air penetration decreased as canopy density increased. The airflow to the targeted tree decreased as the air inlet diameter decreased. The damper opening 2 offered higher spray coverage on high-density trees than the other openings. However, this opening was not suitable for spraying medium-density and low-density trees. The damper opening 4 could be suitable for medium-density fruit trees and opening 5 for low-density trees. These recommendations were made based on calculated tree canopy points in the month of June. When the tree canopy points are increased, the recommendations might need to be reconsidered. The airflow control system was able to calculate the required damper opening and the airflow requirement for uniform spray coverage and reduced drift compared to traditional precision airblast sprayers used in tree fruit orchards and performed the function in real-time based on average tree canopy density from ten consecutive trees.

Even though the system had the capability of changing airflow based on tree canopy densities, the slow mechanical motions of the airflow regulator limited the control based on individual trees. However, this system can control airflow for future precision or variable rate airblast sprayers for tree fruit orchards, which demonstrates the potential of using this system for successful spray applications.

Acknowledgments

This study was supported in part by the United States Department of Agriculture (USDA)'s National Institute of Food and Agriculture (NIFA) Federal Appropriations under Project PEN04653 and Accession No. 1016510, a USDA NIFA Crop Protection and Pest Management Program (CPPM) competitive grant (Award No. 2019-70006-30440), and Northeast Sustainable Agriculture Research and Education (SARE) Graduate Student Grant GNE20-234-34268.

References

Barbedo, J. G. (2019). Detection of nutrition deficiencies in plants using proximal images and machine learning: A review. *Comput. Electron. Agric., 162*, 482-492. https://doi.org/10.1016/j.compag.2019.04.035

Béland, M., & Kobayashi, H. (2021). Mapping forest leaf area density from multiview terrestrial lidar. *Methods Ecol. Evol., 12*(4), 619-633. https://doi.org/10.1111/2041-210X.13550

Berk, P., Hocevar, M., Stajnko, D., & Belsak, A. (2016). Development of alternative plant protection product application techniques in orchards, based on measurement sensing systems: A review. *Comput. Electron. Agric., 124*, 273-288. https://doi.org/10.1016/j.compag.2016.04.018

Berk, P., Stajnko, D., Belsak, A., & Hocevar, M. (2020). Digital evaluation of leaf area of an individual tree canopy in the apple orchard using the LIDAR measurement system. *Comput. Electron. Agric., 169*, 105158. https://doi.org/10.1016/j.compag.2019.105158

Boatwright, H., Zhu, H., Clark, A., & Schnabel, G. (2020). Evaluation of the intelligent sprayer system in peach production. *Plant Disease, 104*(12), 3207-3212. https://doi.org/10.1094/pdis-04-20-0696-re

Cai, J., Wang, X., Gao, Y., Yang, S., & Zhao, C. (2019). Design and performance evaluation of a variable-rate orchard sprayer based on a laser-scanning sensor. *Int. J. Agric. Biol. Eng., 12*(6), 51-57. https://doi.org/10.25165/j.ijabe.20191206.4174

Cerruto, E., Manetto, G., Longo, D., Failla, S., & Papa, R. (2019). A model to estimate the spray deposit by simulated water sensitive papers. *Crop Prot., 124*, 104861. https://doi.org/10.1016/j.cropro.2019.104861

Chen, Y., Zhu, H., & Ozkan, H. E. (2012). Development of a variable-rate sprayer with laser scanning sensor to synchronize spray outputs to tree structures. *Trans. ASABE, 55*(3), 773-781. https://doi.org/10.13031/2013.41509

Colaço, A. F., Molin, J. P., Rosell-Polo, J. R., & Escolà, A. (2018). Application of light detection and ranging and ultrasonic sensors to high-throughput phenotyping and precision horticulture: current status and challenges. *Hortic. Res., 5*. https://doi.org/10.1038/s41438-018-0043-0

Colaço, A. F., Molin, J. P., Rosell-Polo, J. R., & Escolà, A. (2019). Spatial variability in commercial orange groves. Part 1: Canopy volume and height. *Precis. Agric., 20*(4), 788-804. https://doi.org/10.1007/s11119-018-9612-3

Escolà, A., Rosell-Polo, J. R., Planas, S., Gil, E., Pomar, J., Camp, F.,... Solanelles, F. (2013). Variable rate sprayer. Part 1 –

Orchard prototype: Design, implementation and validation. *Comput. Electron. Agric., 95*, 122-135. https://doi.org/10.1016/j.compag.2013.02.004

Fox, R. D., Derksen, R. C., Zhu, H., Brazee, R. D., & Svensson, S. A. (2008). A history of air-blast sprayer development and future prospects. *Trans. ASABE, 51*(2), 405-410. https://doi.org/10.13031/2013.24375

Gu, J., Zhu, H., & Ding, W. (2012). Unimpeded air velocity profiles of an air-assisted five-port sprayer. *Trans. ASABE, 55*(5), 1659-1666. https://doi.org/10.13031/2013.42350

Gu, J., Zhu, H., Ding, W., & Wang, X. (2014). Characterization of air profiles impeded by plant canopies for a variable-rate air-assisted sprayer. *Trans. ASABE, 57*(5), 1307-1315. https://doi.org/10.13031/trans.57.10646

Hu, M., & Whitty, M. (2019). An evaluation of an apple canopy density mapping system for a variable-rate sprayer. *IFAC-PapersOnLine, 52*(30), 342-348. https://doi.org/10.1016/j.ifacol.2019.12.563

Jeon, H. Y., & Zhu, H. (2012). Development of a variable-rate sprayer for nursery liner applications. *Trans. ASABE, 55*(1), 303-312. https://doi.org/10.13031/2013.41240

Khodabakhshian, R., & Javadpour, S. M. (2021). Design and development of a sensor-based precision crop protection autonomous system for orchard sprayer. *Agric. Eng. Int.: CIGR J., 23*(3).

Liu, H., & Zhu, H. (2016). Evaluation of a laser scanning sensor in detection of complex-shaped targets for variable-rate sprayer development. *Trans. ASABE, 59*(5), 1181-1192. https://doi.org/10.13031/trans.59.11760

Llorens, J., Gil, E., Llop, J., & Escolà, A. (2010). Variable rate dosing in precision viticulture: Use of electronic devices to improve application efficiency. *Crop Prot., 29*(3), 239-248. https://doi.org/10.1016/j.cropro.2009.12.022

Mahmud, M. S., Zahid, A., He, L., Choi, D., Krawczyk, G., & Zhu, H. (2021b). LiDAR-sensed tree canopy correction in uneven terrain conditions using a sensor fusion approach for precision sprayers. *Comput. Electron. Agric., 191*, 106565. https://doi.org/10.1016/j.compag.2021.106565

Mahmud, M. S., Zahid, A., He, L., Choi, D., Krawczyk, G., Zhu, H., & Heinemann, P. (2021a). Development of a LiDAR-guided section-based tree canopy density measurement system for precision spray applications. *Comput. Electron. Agric., 182*, 106053. https://doi.org/10.1016/j.compag.2021.106053

Marucco, P., Tamagnone, M., & Balsari, P. (2008). Study of air velocity adjustment to maximise spray deposition in peach orchards. *Agric. Eng. Int.: CIGR J.*

Owen-Smith, P., Perry, R., Wise, J., Jamil, R. Z., Gut, L., Sundin, G., & Grieshop, M. (2019). Spray coverage and pest management efficacy of a solid set canopy delivery system in high density apples. *Pest Manag. Sci., 75*(11), 3050-3059. https://doi.org/10.1002/ps.5421

Pai, N., Salyani, M., & Sweeb, R. D. (2009). Regulating airflow of orchard airblast sprayer based on tree foliage density. *Trans. ASABE, 52*(5), 1423-1428. https://doi.org/10.13031/2013.29122

Palleja, T., & Landers, A. J. (2015). Real time canopy density estimation using ultrasonic envelope signals in the orchard and vineyard. *Comput. Electron. Agric., 115*, 108-117. https://doi.org/10.1016/j.compag.2015.05.014

Partel, V., Costa, L., & Ampatzidis, Y. (2021). Smart tree crop sprayer utilizing sensor fusion and artificial intelligence. *Comput. Electron. Agric., 191*, 106556. https://doi.org/10.1016/j.compag.2021.106556

Pivato, A., Barausse, A., Zecchinato, F., Palmeri, L., Raga, R., Lavagnolo, M. C., & Cossu, R. (2015). An integrated model-based approach to the risk assessment of pesticide drift from vineyards. *Atmos. Environ., 111*, 136-150. https://doi.org/10.1016/j.atmosenv.2015.04.005

Salyani, M., & Fox, R. D. (1999). Evaluation of spray quality by oiland water-sensitive papers. *Trans. ASAE, 42*(1), 37-43. https://doi.org/10.13031/2013.13206

Seol, J., Kim, J., & Son, H. I. (2022). Field evaluations of a deep learning-based intelligent spraying robot with flow control for pear orchards. *Precis. Agric., 23*(2), 712-732. https://doi.org/10.1007/s11119-021-09856-1

Torr, P.H. & Zisserman, A. (2000). MLESAC: A new robust estimator with application to estimating image geometry. Computer vision and image understanding, 78(1), 138-156. https://doi.org/10.1006/cviu.1999.0832

Tumbo, S. D., Salyani, M., Whitney, J. D., Wheaton, T. A., & Miller, W. M. (2002). Investigation of laser and ultrasonic ranging sensors for measurements of citrus canopy volume. *Appl. Eng. Agric., 18*(3), 367. https://doi.org/10.13031/2013.8587

Wei, J., & Salyani, M. (2005). Development of a laser scanner for measuring tree canopy characteristics: Phase 2. Foliage density measurement. *Trans. ASAE, 48*(4), 1595-1601. https://doi.org/10.13031/2013.19174

Zhang, Z., Wang, X., Lai, Q., & Zhang, Z. (2018). Review of variable-rate sprayer applications based on real-time sensor technologies. In S. Hussmann (Ed.), *Automation in agriculture: Securing food supplies for future generations* (pp. 53-79). https://doi.org/10.5772/intechopen.73622

Zhu, H., Derksen, R. C., Guler, H., Krause, C. R., & Ozkan, H. E. (2006). Foliar deposition and off-target loss with different spray techniques in nursery applications. *Trans. ASABE, 49*(2), 325-334. https://doi.org/10.13031/2013.20400

Zhu, H., Salyani, M., & Fox, R. D. (2011). A portable scanning system for evaluation of spray deposit distribution. *Comput. Electron. Agric., 76*(1), 38-43. https://doi.org/10.1016/j.compag.2011.01.003

Zhu, H., Zondag, R. H., Derksen, R. C., Reding, M., & Krause, C. R. (2008). Influence of spray volume on spray deposition and coverage within nursery trees. *J. Environ. Hortic., 26*(1), 51-57. https://doi.org/10.24266/0738-2898-26.1.51

APPENDIX

Input: scanned lidar frame

Output: steps, direction

initialize lidar
initialize arduino
initial damper position, $\mathbf{D_p} \longleftarrow 0$
frames ⟵ readframe(lidar)
for each data i **in** frames **do**
  point cloud, $\mathbf{P_c} \longleftarrow$ get a new frame started with data i (frames, i)
  transformation, $\mathbf{TM_{pc}} \longleftarrow$ transform point cloud to oriented like real tree (P_c)
  tree points, $\mathbf{T_{pc}} \longleftarrow$ find point cloud within individual tree region of interest (TM_{pc})
  inPlanePointIndices, $\mathbf{I_p} \longleftarrow$ find in plane point indices from the tree points (T_{pc})
  outliers, $\mathbf{O_p} \longleftarrow$ find outlier points from the segmented tree points (T_{pc})
  ground point clouds, $\mathbf{G_{pc}} \longleftarrow$ find ground points based on T_{pc} and I_p
  tree canopy points without ground, $\mathbf{T_{pwc}} \longleftarrow$ calculate after removing outliers (O_p)
  final tree point indices, $\mathbf{F_{tp}} \longleftarrow$ select the remaining points within tree region of interest
  number of canopy points, $\mathbf{N_{cp}} \longleftarrow$ count number of canopy points of each tree
  if $N_{cp} > 5000$ **then** (for high density, $N_{cp} > 1000$)
    canopy points, $\mathbf{C_p} \longleftarrow N_{cp}$ (this if statement will help to exclude open area between trees)
  end if
  i ⟵ i + 5
end for
  total canopy points, $\mathbf{TC_p} \longleftarrow$ summation of all canopy points from captured trees
  average canopy points, $\mathbf{AC_p} \longleftarrow TC_p$ divide with number of frame captured
  damper opening, $\mathbf{D_{op}} \longleftarrow$ calculate from developed model using tree canopy points
  motor steps, $\mathbf{M_{st}} \longleftarrow$ calculate from developed model using damper opening
  if $D_p = 0$ **then**
    required damper position, $\mathbf{D_{rp}} \longleftarrow \mathbf{M_{st}}$
  else
    $\mathbf{D_{rp}} \longleftarrow$ subtraction from motor steps and D_p
  end if
  if $D_{rp} > 0$ **and** $D_{rp} < 29000$ **then**
    steps ⟵ D_{rp}
    direction ⟵ clockwise
  end if
  steps, direction ⟵ send to arduino through serial communication
  Remove all processed information

Figure A1. Algorithm for automatic damper control in the orchard condition scripted in MATLAB®.